Inorg. Chem. **2007**, *46*, 4660–4666

Inorganic Chemistry
Article

New Functional Model Complexes of Intradiol-Cleaving Catechol Dioxygenases: Properties and Reactivity of $Cu^{II}(L)(O_2Ncat)$

József Kaizer,[†] Zoltán Zsigmond,[†] Ildikó Ganszky,[†] Gábor Speier,*[,†] Michel Giorgi,[‡] and Marius Réglier[‡]

Department of Organic Chemistry, University of Pannonia, 8201 Veszprém, Hungary, and Laboratoire de Cristallochimie et Laboratoire de Bioinorganique Structurale, Université Paul Cézanne Aix-Marseille III F.S.T. Saint-Jerôme, Service 432 Avenue Escadrille Normandie-Niemen, 13397 Marseille Cedex 20, France

Received December 4, 2006

Complexes $Cu(O_2Ncat)(tbeda)$ (**1**) and $Cu(O_2Ncat)(tmeda)$ (**2**) (tbeda = *N*,*N*,*N*′,*N*′-tetrabenzylethylenediamine, tmeda = *N*,*N*,*N*′,*N*′-tetramethylethylenenediamine, O_2NcatH_2 = 4-nitrocatechol) have been prepared by the reaction of copper(II) perchlorate with 4-nitrocatechol in the presence of triethylamine and the appropriate bidentate ligand. These compounds represent structural and functional model systems for the copper-containing catechol 1,2-dioxygenase. Both complexes have been structurally characterized by X-ray crystallography and by UV–vis, IR, and EPR spectroscopies. Upon protonation of **1** and **2** with perchloric acid, the bidentate coordination of O_2-Ncat could be reversible converted to the monodentate coordination of O_2NcatH. The equilibrium constants were found to be 4200 and 3500, respectively, by measuring the UV–vis spectra in DMF. Back-titration with morpholine proved the reversibility of both reactions. Kinetic data on the oxygenation of **1** and **2** revealed overall second-order rate equations with kinetic parameters: $k_{tbeda} = (4.63 \pm 0.23) \times 10^{-2}$ mol^{-1} dm^3 s^{-1}, $\Delta H^{\ddagger} = 51 \pm 6$ kJ mol^{-1}, $\Delta S^{\ddagger} = -137 \pm 16$ J mol^{-1} K^{-1}; $k_{tmeda} = (0.89 \pm 0.23)$ mol^{-1} dm^3 s^{-1}, $\Delta H^{\ddagger} = 85 \pm 7$ kJ mol^{-1}, $\Delta S^{\ddagger} = -57 \pm 19$ J mol^{-1} K^{-1} at 365.16 K. Oxygenation of **1**, **2**, and $[Cu(O_2NcatH)(L)]ClO_4$ (L = tbeda, tmeda) in DMF solution at ambient conditions gives the corresponding intradiol ring-cleaved (2-nitro-muconato)copper(II) complexes. These data support the assumption that the reaction of the differently coordinated catecholate ligand with dioxygen shows only 1,2-dioxygenase activity.

Introduction

Aerobic microorganisms play an important role in the oxidative degradation of aromatic compounds.[1–5] The aromatic rings are first hydroxylated to phenols or diphenols, either through successive steps or dihydroxylation, which are the key compounds for either oxidation by dioxygen to *o*-quinones catalyzed by catechol oxidases,[6–8] as shown in a in Scheme 1, or dioxygenation by molecular oxygen to ring-cleaved products by catechol dioxygenases.[9] The catechol oxidase enzymes contain two copper ions at their active site.[6] The catalytic cleavage of catechols yields aliphatic products by insertion of both atoms of dioxygen into the aromatic ring.[10–13] Traditionally, catechol dioxygenases are subdivided into intradiol- and extradiol-cleaving enzymes according to their catalysis of the ring cleavage between or

* To whom correspondence should be addressed. E-mail: speier@almos.vein.hu. Fax: +36-88/62-4469.
[†] Pannon University.
[‡] Université Paul Cézanne Aix-Marseille III F.S.T. Saint-Jerôme.

(1) Bugg, T. D. *Chem. Commun*. **2001**, 941.
(2) Gibson, D. T. *Microbial Degradation of Organic Molecules*; Dekker: New York, 1984.
(3) Bugg, T. D.; Voisin, J. S.; Spence, E. L. *Biochem. Soc. Trans*. **1997**, *25*, 81.
(4) Lipscomb, J. D.; Orville, A. M. *Met. Ions Biol. Syst*. **1992**, *28*, 243.
(5) Que, L., Jr.; Reynolds, M. F. *Met. Ions Biol. Syst*. **2000**, *37*, 505.
(6) Klabunde, T.; Eicken, C.; Sacchettini, J. C.; Krebs, B. *Nat. Struct. Biol*. **1998**, *5*, 1084.
(7) Eicken, C.; Zippel, F.; Büldt-Karentzopoulos, K.; Krebs, B. *FEBS Lett*. **1998**, *436*, 293.
(8) Eicken, C.; Krebs, B.; Sacchettini, J. C. *Curr. Opin. Struct. Biol*. **1999**, *9*, 677.
(9) Que, L., Jr.; Ho, R. Y. N. *Chem. Rev*. **1996**, *96*, 2607.
(10) Senda, T.; Sygiyama, K.; Narita, H.; Yamamoto, T.; Kimbara, K.; Fukuda, M.; Sato, M.; Yano, K.; Mitsui, Y. *J. Mol. Biol*. **1996**, *255*, 735.
(11) Ohlendorf, D. H.; Lipscomb, J. D.; and Weber, P. C. *Nature (London)* **1988**, *336*, 403.
(12) Que, L., Jr. *Iron Carriers and Iron Proteins*; Loehr, T. M., Ed.; VCH: New York, 1989.
(13) Lange, S. J.; Que, L., Jr. *Curr. Opin. Chem. Biol*. **1998**, *2*, 159.

10.1021/ic062309a CCC: $37.00
Published on Web 04/26/2007

Scheme 1

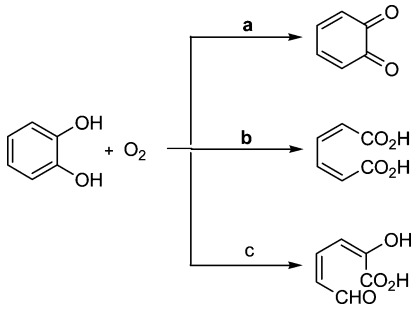

outside the two *ortho*-hydroxo groups.[14] The intradiol-cleaving catechol dioxygenases (b in Scheme 1) contain an Fe(III)[15−18] or Cu(II),[19] while in contrast, the extradiol-cleaving catechol dioxygenases (c in Scheme 1) typically contain an Fe(II) active site.[3−5,20−22] However, Mn(II)-dependent extradiol-cleaving enzymes have also been characterized,[23−25] and in one case, a Mg(II)-dependent extradiol-cleaving catechol dioxygenase has been reported.[26]

In previous studies, several functional models have been synthesized to gain insight into the mechanism of catechol cleavage.[27−30] Complexes of copper have appeared prominently in these investigations.[31−34] Questions regarding the mechanism of dioxygen activation, stereoselectivity, and intra- versus extradiol ring cleavage remain as subjects of investigation. Earlier models have shown that the dioxygenase activity strongly depends on the nature of the ligand set and the coordination mode of the catecholate ligand.[35−39] 4-Nitrocatechol binding studies on iron and manganese model systems suggest that the extradiol-cleaving catechol dioxygenases selectively favor the monoanionic state of catechol, in contrast to the intradiol enzymes which bind catechol as a dianion.[40] Here we describe several new copper(II) catecholate complexes as model compounds for catechol 1,2-dioxygenases with the chromophoric probe 4-nitrocatechol and various bidentate ligands. The steric and electronic influence of the nitrogen-donor ligand set and the effect of the binding mode of the 4-nitrocatechol on the biomimetic catechol 1,2-dioxygenase activity is probed with spectroscopic and functional investigations on the prepared copper(II) compounds.

Experimental Section

General Remarks. Solvents used for the reactions were purified using literature methods[41] and stored under argon. The ligands *N*,*N*,*N*′,*N*′-tetramethylethylenediamine and 4-nitrocatechol (Aldrich) were used as provided. All air-sensitive compounds were handled under argon using standard Schlenk techniques.[42] ***Caution:*** *Perchlorate salts of metal complexes with organic ligands are potentially explosive. Only small amounts of material should be prepared, and these should be handled with great care!* Infrared spectra were recorded on a Specord 75 IR (Carl Zeiss) spectrophotometer using samples mulled in Nujol between KBr plates or in KBr pellets. UV−vis spectra were recorded on a Shimadzu UV-160 spectrophotometer using quartz cells. The EPR spectra were recorded at room temperature by an X-band Bruker Elexsys 500 spectrometer. GC analyses were performed on a HP 5830A gas chromatograph equipped with a flame ionization detector. Analyses were performed on a HP 5890II/5971 GC/MSD apparatus equipped with a column identical to that used for GC analyses. Cyclic voltammetry experiments for compounds **1** and **2** in the absence and also in the presence of $HClO_4$ were carried out with a Pt working electrode on a BAS CV-1B cyclic voltammeter in DMF ($\sim 10^{-4}$ M solution) at room temperature with NBu_4ClO_4 as supporting electrolyte and a scan rate 60 mV s^{-1}; the potential values are relative to the saturated calomel electrode (SCE) using an Ag−AgCl reference electrode (Figure S1). Microanalyses were done by the Microanalytical Service of the Pannon University.

***N*,*N*,*N*′,*N*′-Tetrabenzylethylenediamine (tbeda).** Benzyl bromide (15.39 g, 0.09 mol) and then benzylethylenediamine (4.5 g, 0.03 mol) were added slowly to 90 mL of water under cooling. A KOH (15 mL, 6 M) solution was then added to the stirred solution, along with an additional 2−3 mL of acetonitrile. The mixture was left overnight, and the pink crystals were filtered, dissolved in ether, dried over $MgSO_4$, and concentrated under vacuum to give colorless crystals (6.3 g, 50%). Mp: 91 °C. IR (KBr): ν 3081, 3061, 3023, 2946, 2791, 2708, 1493, 1451, 1371, 1363, 1234, 1122, 1088, 1066,

(14) Que, L., Jr. In *Bioinorganic Catalysis*, 2nd. ed.; Reedijk, J., Bouwman, Eds.; New York, Basel, 1999.
(15) Kent, T. A.; Münck, E.; Pyrz, J. W.; Widom, J.; Que, L., Jr. *Inorg. Chem.* **1987**, *26*, 1402.
(16) Nakazawa, T.; Kojima, Y.; Fujisawa, H.; Nozaki, M.; Hayaishi, O.; Yamano, T. *J. Biol. Chem.* **1965**, *240*, PC3224.
(17) Nakami, K.; Miyake, Y. *Biochem. Biophys. Res. Commun.* **1971**, *42*, 497.
(18) Bull, C.; Ballou, D. P.; Otsuka, S. *J. Biol. Chem.* **1981**, *256*, 12681.
(19) Sharma, H. K.; Vaidyanathan, C. S. *Eur. J. Biochem.* **1975**, *56*, 163.
(20) Hegg, E. L.; Que, L., Jr. *Eur. J. Biochem.* **1997**, *250*, 625.
(21) Que, L. Jr. *Nat. Struct. Biol.* **2000**, *7*, 182.
(22) Shu, L.; Chiou, Y.-M.; Orville, A. M.; Miller, M. A.; Lipscomb, J. D.; Que, L. Jr. *Biochemistry* **1995**, *34*, 6649.
(23) Que, L., Jr.; Widom, J.; Crawford, R. L. *J. Biol. Chem.* **1981**, *256*, 10941.
(24) Boldt, Y. R.; Sadowsky, M.; Ellis, L. B. M.; Que, L., Jr.; Wackett, L. P. *J. Bacteriol.* **1995**, *177*, 1225.
(25) Whiting, A. K.; Boldt, Y. R.; Hendrich, M. P.; Wackett, L. P.; Que, L., Jr. *Biochemistry* **1996**, *35*, 160.
(26) Gibello, A.; Ferrer, E.; Martin, M.; Garrido-Pertierra, A. *Biochem. J* **1994**, *301*, 145.
(27) Jang, H. G.; Cox, D. D.; Que, L., Jr. *J. Am. Chem. Soc.* **1991**, *113*, 9200.
(28) Koch, W. O.; Krüger, H. -J. *Angew. Chem.* **1995**, *107*, 2929.
(29) Chiou, Y.-M.; Que, L., Jr. *Inorg. Chem.* **1995**, *34*, 3577.
(30) Mialane, P.; Tchertanov, L.; Banse, F.; Sainton, J.; Girerd, J.-J. *Inorg. Chem.* **2000**, *39*, 2440.
(31) Speier, G.; Tyeklár, Z.; Tóth, P.; Speier, E.; Tisza, S.; Rockenbauer, A.; Whalen, A. M.; Alkire, N.; Pierpont, C. G. *Inorg. Chem.* **2001**, *40*, 5653.
(32) Speier, G.; Tisza, S.; Rockenbauer, A.; Boone, S. R.; Pierpont, C. G. *Inorg. Chem.* **1992**, *31*, 1017.
(33) Speier, G.; Tyeklár, Z.; Szabó, L.; Tóth, P., II; Pierpont, C. G.; Hendrickson, D. N. In *The Activation of Dioxygen and Homogeneous Catalytic Oxidation*; Barton, D. H. R., Martell, A. E., Sawyer, D. T., Eds.; Plenum Press: New York, 1993; pp. 423−436.
(34) Brown, D. G.; Beckmann, L.; Ashby, C. H.; Vogel, G. C.; Reinprecht, J. T. *Tetrahedron Lett.* **1977**, 1363.
(35) Pascaly, M.; Duda, M.; Rompel, A.; Sift, B. H.; Meyer-Klaucke, W.; Krebs, B. *Inorg. Chim. Acta* **1999**, *291*, 289.
(36) Pascaly, M.; Nazikkol, C.; Schweppe, F.; Wiedemann, A.; Zurlinden, K.; Krebs, B. *Z. Anorg. Allg. Chem.* **2000**, *626*, 50.
(37) Nishida, Y.; Shimo, H.; Kida, S. *J. Chem. Soc., Chem. Commun.* **1994**, 1611.
(38) Viswanathan, R.; Palaniandavar, M.; Balasubramanian, T.; Mutiah, T. P. *Inorg. Chem.* **1999**, *37*, 2943.
(39) Pascaly, M.; Duda, M.; Schweppe, F.; Zurlinden, K.; Müller, F. K.; Krebs, B. *J. Chem. Soc., Dalton Trans.* **2001**, 828.
(40) Reynolds, M. F.; Costas, M.; Ito, M.; Jo, D.-H.; Tipton, A.; Whiting, A. K.; Que, L., Jr. *J. Biol. Inorg. Chem.* **2003**, *8*, 263.
(41) Perrin, D. D.; Armarego, W. L.; Perrin, D. R. *Purification of Laboratory Chemicals*, 2nd ed.; Pergamon: New York, 1990.
(42) Shriver, D. F.; Drezdzon, M. A. *The Manipulation of Air-sensitive Compounds*; John Wiley & Sons: New York, 1986.

Table 1. Crystal Data and X-ray Experimental Parameters for Complexes $Cu^{II}(O_2Ncat)(tbeda)$ (**1**) and $Cu^{II}(O_2Ncat)(tmeda)$ (**2**)

	1	**2**
empirical formula	$C_{36}H_{36}Cu_1N_3O_{4.5}$	$C_{12}H_{19}Cu_1N_3O_4$
molecular mass	646.2	332.84
temp	293(2) K	293(2) K
cryst syst	monoclinic	monoclinic
space group	$C2/c$	$P2_1/c$
a (Å)	35.118(4)	8.4292(6)
b (Å)	10.999(2)	11.9941(9)
c (Å)	18.437(3)	15.952(1)
α (deg)	90	90
β (deg)	114.890(10)	115.337(5)
γ (deg)	90	90
vol. (Å^3)	6460.1(17)	1457.62(18)
Z	8	4
density (calcd) (Mg m^{-3})	1.328	1.517
abs coeff, μ (mm^{-1})	0.721	1.514
F(000)	2700	692
cryst size (mm)	0.80 × 0.12 × 0.03	0.30 × 0.30 × 0.20
θ range [deg]	$1.28 \le \theta \le 28.11$	$2.21 \le \theta \le 24.67$
index ranges	$0 \le h \le 46$	$-9 \le h \le 9$
	$0 \le k \le 14$	$-14 \le k \le 14$
	$-21 \le l \le 19$	$-18 \le l \le 1$
final R indices [$I > 2\sigma(I)$]	R1 = 0.1022	R1 = 0.0650
	wR2 = 0.2096	wR2 = 0.1892
R indices (all data)	R1 = 0.1921	R1 = 0.0764
	wR2 = 0.2590	wR2 = 0.2101
max. and mean shift (esd)	0.001, 0.000	0.000, 0.000
largest diff. peak and hole (e· Å^{-3})	0.928 and −0.516	0.901 and −0.808

1028, 977, 969, 743, 731, 694, 470 cm^{-1}. ^{1}H NMR ($CDCl_3$): δ 2.6 (s, 4H), δ 3.55 (s, 8H), δ 7.1−7.4 (m, 20H). Anal. Calcd (found) for $C_{30}H_{32}N_2$ (420.6): C, 85.67 (86.06); H, 7.67 (7.89); N, 6.66 (6.68).

Preparation of $Cu^{II}(O_2Ncat)(tbeda)$ (1). $Cu(ClO_4)_2{\cdot}6H_2O$ (686.3 mg, 1.85 mmol), tbeda (778 mg, 1.85 mmol), and 4-nitrocatechol (287 mg, 1.85 mmol) were dissolved in methanol (5 mL); triethylamine (0.26 mL) was then added dropwise, and the solution was stirred under argon for 20 h. A brown solid formed, which was filtered, washed two times with methanol, and dried under vacuum (0.85 g, 72%). The product was recrystallized from CH_2Cl_2 by ether addition. Mp: 164−167 °C. IR (KBr): ν 3033, 2941, 1559, 1496, 1471, 1384, 1270, 1224, 1118, 1072, 796, 735, 699 cm^{-1}. UV−vis (DMF): λ_{max} (ϵ) 283 (8709), 338 (9120), 440 nm (8511 L mol^{-1} cm^{-1}). Anal. Calcd (found) for $C_{36}H_{35}CuN_3O_4$ (637.2): C, 67.85 (67.32); H, 5.54 (5.49); N, 6.59(6.48). EPR (MeCN): g = 2.0973, A_{Cu} = 90.0 G.

Preparation of $Cu^{II}(O_2Ncat)(tmeda)$ (2). Complex **2** was prepared by the method described above for the preparation of **1**. Yield: 0.82 g (49%). The product was recrystallized from THF by ether addition. Mp: 205 °C (dec). IR (KBr): ν 3012, 2987, 2917, 1552, 1505, 1465, 1410, 1350, 1318, 1287, 1271, 1241, 1219, 1201, 1119, 1075, 1022, 953, 857, 808, 737, 641 cm^{-1}. UV−vis (MeCN): λ_{max} (ϵ) 283 (19 055), 346 (4677), 460 nm (11 749 L mol^{-1} cm^{-1}). Anal. Calcd (found) for $C_{12}H_{19}CuN_3O_4$ (332.8): C, 43.30 (43.21); H, 5.75 (5.56); N, 12.62 (12.50). EPR (MeCN): g = 2.1005, A_{Cu} = 87.6 G.

Spectrophotometric Titrations of $Cu^{II}(O_2Ncat)(L)$ (1, 2) with $HClO_4$. The titrations of complexes **1** and **2** were performed by the addition of aqueous $HClO_4$ (66%) in DMF to anaerobic solutions of the dianionic metal complexes via a gastight syringe to form the corresponding monoanionic metal complexes. Ten milliliters of each complex (0.157 mM) in DMF solution was titrated stepwise (100 μL = 0.2 equiv) with a DMF solution of $HClO_4$ (3.142 mM), and the absorbances in the range of 200−600 nm were measured under inert conditions. Back-titrations with a DMF solution of NEt_3 was carried out in a similar manner.

Oxygenations of Complexes $Cu^{II}(O_2Ncat)(L)$ (1, 2). The (catecholato)copper(II) complexes (300 mg) were dissolved in 10 mL of DMF, and the solutions were stirred under dioxygen in the presence or absence of $HClO_4$ for 40 h at 110 °C. The solutions were concentrated to dryness; 10 mL aqueous of H_2SO_4 (10 m/m %) was added to the residue, and the mixtures were extracted by Et_2O (20 mL × 5). The extracts collected were concentrated to dryness to afford oily residues, and their GC-MS analyses after treatment of ethereal diazomethane showed that in both cases the intradiol ring-cleaved product 4-nitromuconic acid and its amidated products are the major products (Figures S3−S5): 2-(2,5-dihydro-2-nitro-5-oxofuran-2-yl)-*N*,*N*-dimethylacetamide (MS, m/z = 214 [M$^+$]), 3-nitro-muconic-acid-(*N*,*N*-dimethyl)-mono-amide-mono-methylester (MS, m/z = 228 [M$^+$]), and 3-nitro-muconic-acid-(*N*,*N*,*N*′,*N*′-tetramethyl-diamide) (MS, m/z = 241 [M$^+$]).

Kinetic Experiments. Reactions of $Cu^{II}(O_2Ncat)(tbeda)$ (**1**) and $Cu^{II}(O_2Ncat)(tmeda)$ (**2**) with dioxygen were performed in DMF solutions (Tables S1 and S2). In a typical experiment, $Cu^{II}(O_2Ncat)$-(tbeda) (**1**) or $Cu^{II}(O_2Ncat)(tmeda)$ (**2**) was dissolved under argon in a thermostatically controlled reaction vessel with an inlet for taking samples with a syringe, connected to a mercury manometer to maintain a constant pressure. The solution was then heated to the appropriate temperature. A sample was then taken by syringe, and the initial concentration of $Cu^{II}(O_2Ncat)(tbeda)$ (**1**) or $Cu^{II}(O_2$-$Ncat)(tmeda)$ (**2**) was determined by UV−vis spectroscopy by measurement the absorbance of the reaction mixture at 440 or 460 nm (λ_{max} of a typical band of $Cu^{II}(O_2Ncat)(tbeda)$ (**1**) or $Cu^{II}(O_2$-$Ncat)(tmeda)$ (**2**)), respectively. The argon was then replaced by dioxygen and consumption of the latter was periodically monitored. The rate of oxygenation was independent of the stirring rate, excluding eventual diffusion control effects. The dioxygen concentrations was calculated from literature data[43] taking into account the partial pressure of DMF,[44] and assuming the validity of Dalton's law.

X-ray Crystallographic Studies. Crystallographic and experimental details of the data collection and refinement of the structures of $Cu^{II}(O_2Ncat)(tbeda)$ (**1**) and $Cu^{II}(O_2Ncat)(tmeda)$ (**2**) are reported in Table 1, while the molecular structures are depicted in Figures 1 and 2. The intensity data of **1** and **2** were collected with a KappaCCD single-crystal diffractometer, using the graphite-monochromated Mo Kα radiation. The structures were solved by direct and difmap methods (SIR92),[45] and refined by SHELXL-97[46] program. CCDC-629155 (**1**) and 629154 (**2**) contain the supplementary crystallographic data for this paper.

Results and Discussion

Synthesis and Characterization of $Cu^{II}(L)(O_2Ncat)$. Complexes $Cu^{II}(O_2Ncat)(tbeda)$ (**1**) and $Cu^{II}(O_2Ncat)(tmeda)$ (**2**) were isolated as green solids by the reaction of $Cu(ClO_4)_2{\cdot}6H_2O$, 4-nitrocatechol, and the corresponding coligands tmeda or tbeda in the presence of NEt_3 at room temperature in methanol under argon. Satisfactory elemental analyses were obtained for both complexes, which have very similar

(43) Kruis, A. *Landolt-Börnstein*; Springer-Verlag: Berlin, 1976; Board 4, Teil 4.
(44) Ram, G.; Sharaf, A. R. *J. Indian Chem. Soc.* **1968**, *45*, 13.
(45) Sheldrick, G. M. *SHELXL97, Program for the Refinement of Crystal Structures*; University of Göttingen: Göttingen, Germany, 1997.
(46) Altomare, A.; Cascarano, G.; Giacovazzo, C.; Guagliardi, A.; Burla, M. C.; Polidori, G.; Camalli, M. *J. Appl. Crystallogr.* **1994**, *27*, 435.

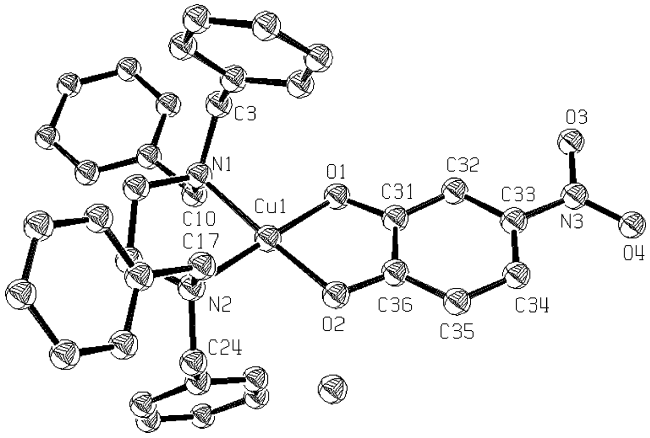

Figure 1. Crystal structure of the $Cu^{II}(O_2Ncat)(tbeda)\cdot H_2O$ (**1**) complex showing 50% probability thermal ellipsoids. Hydrogen atoms are omitted for clarity.

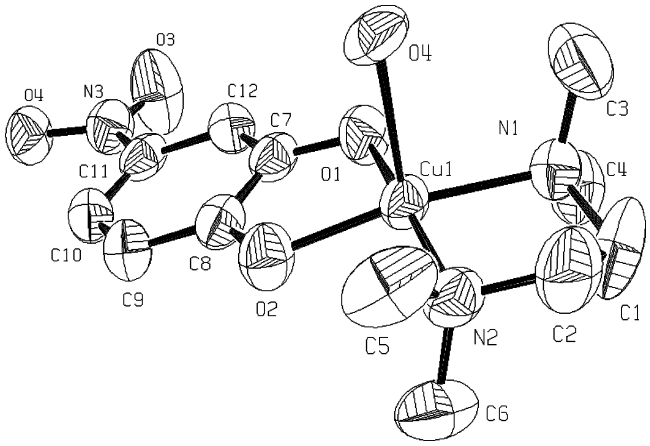

Figure 2. Crystal structure of the $Cu^{II}(O_2Ncat)(tmeda)\cdot H_2O$ (**2**) complex showing 50% probability thermal ellipsoids. Hydrogen atoms are omitted for clarity.

Table 2. Properties of the $Cu^{II}(O_2Ncat)(tbeda)$ (**1**) and $Cu^{II}(O_2Ncat)(tmeda)$ (**2**) Complexes

complex	λ_{max}[a] (nm)	ν_{CO}[b] (cm^{-1})	K_H[c] (mol^{-1} dm^3)	$E_{1/2}$ (mV)
1	440	1270, 1471	4169	−50
2	460	1271, 1465	3467	223

[a] In DMF. [b] KBr. [c] Titration with $HClO_4$.

IR and electronic spectra. Their IR spectrum shows principal bands corresponding to the coordinated 4-nitrocatecholate (O_2Ncat) at 1270, 1471 and 1271, 1465 cm^{-1}, respectively. The charge-transfer region in the electronic spectra of the complexes $Cu^{II}(O_2Ncat)(tbeda)$ and $Cu^{II}(O_2Ncat)(tmeda)$ exhibit bands of the coordinated 4-nitrocatecholate ligand at 440 and 460 nm (Table 2). The difference in charge distribution for four-coordinate complexes containing phosphine and amine coligands may understood as a σ-bonding effect that raises the copper d_σ orbital energy above the partially occupied semiquinone π orbital. The change in charge distribution results in a consequent shift in the paramagnetic center of the molecule and a shift in the center of nucleophilicity. With soft donors and π-acceptor ligands, the complexes have the $L_2Cu^I(SQ)$ charge distribution.

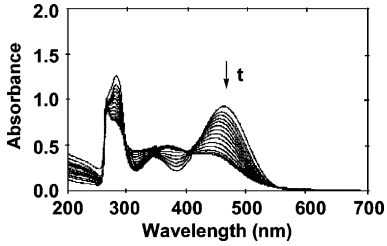

Figure 3. Time sequence of the decrease in the absorption band of $Cu^{II}(O_2Ncat)(tbeda)$ (**1**) during the oxygenation reaction in DMF. $[Cu^{II}(O_2Ncat)(tbeda)] = 0.18$ mM, $[O_2] = 7.95$ mM, 92 °C.

Table 3. Selected Bond Distances and Angles for Complexes $Cu^{II}(O_2Ncat)(tbeda)$ (**1**) and $Cu^{II}(O_2Ncat)(tmeda)$ (**2**)

	1	**2**
Cu1−O1	1.888(5)	1.907(4)
Cu−O2	1.926(5)	1.934(5)
Cu1−N1	2.037(5)	2.049(5)
Cu1−N2	2.020(5)	2.028(6)
O1−C31(C7)	1.346(8)	1.343(7)
O2−C36(C8)	1.307(9)	1.299(8)
O3−N3	1.271(12)	1.229(8)
O4−N3	1.306(13)	1.267(7)
O1−Cu1−O2	86.9(2)	86.43(19)
O1−Cu1−N1	94.5(2)	94.3(2)
N2−Cu1−N1	86.2(2)	86.1(2)
C31(C7)−O1−Cu1	108.7(5)	109.4(4)
C38(8)−O2−Cu1	109.3(5)	110.7(4)

Structural characterization on $(PR_3)_2Cu^I(3,6\text{-DBSQ})$ complexes has shown that the metals have the expected tetrahedral coordination geometry, and EPR spectra are typical of organic radicals weakly coupled with the $^{63,65}Cu$ nuclei.[47] Four-coordinate $L_2Cu^{II}(Cat)$ complexes have been characterized structurally with nitrogen-donor ancillary ligands and found to have square planar geometries.[48] EPR spectra are typical of planar Cu(II) complexes with strong g anisotropy and strong $^{63,65}Cu$ hyperfine coupling.[47] The solution spectrum of $Cu^{II}(O_2Ncat)(tbeda)$ and $Cu^{II}(O_2Ncat)(tmeda)$ complexes recorded in acetonitrile at room temperature consists of a strongly coupled four-line spectrum that is typical of square planar Cu(II) complexes [$g_{iso} = 2.0973$, $A_{iso}(^{63,65}Cu) = 90.0$ G and $g_{iso} = 2.1005$, $A_{iso}(^{63,65}Cu) = 87.6$ G, respectively].[32] Single crystals suitable for X-ray crystallography were obtained upon slow ether diffusion into CH_2Cl_2 and THF solutions of $Cu^{II}(O_2Ncat)(tbeda)$ and $Cu^{II}(O_2Ncat)(tmeda)$, respectively. The molecular structure and selected bond lengths and angles of $Cu^{II}(O_2Ncat)(tbeda)$ are shown in Figure 1 and Table 3. The complex is monomeric and the copper(II) center is in a distored square planar environment.

Crystallographic characterization has shown that in $Cu^{II}(O_2Ncat)(tmeda)$ (Figure 2), the copper(II) ion has a distorted square pyramidal arrangement ($\tau = 0.08$)[49] with basal planes

(47) (a) Kashtanov, E. A.; Cherkasov, V. K.; Gorbunova, L. V.; Abakumov, G. A. *Izv. Akad. Nauk SSSR Ser. Khim.* **1983**, 2121. (b) Rockenbauer, A.; Györ, M.; Speier, G.; Tyeklár, Z. *Inorg. Chem.* **1987**, *26*, 3293. (c) Buchanan, R. M.; Wilson-Blumenberg, C.; Trapp, C.; Larsen, S.; Green, D. L.; Pierpont, C. G. *Inorg. Chem.* **1986**, *25*, 3070. (d) Speier, G. *New J. Chem.* **1994**, *18*, 143.
(48) Pierpont, C. G.; Lange, C. W. *Prog. Inorg. Chem.* **1994**, *41*, 331.
(49) Addison, A. W.; Rao, T. N.; Reedijk, J.; van Rijn, J; Verschoor, G. C. *J. Chem. Soc., Dalton Trans.* **1984**, 1350.

Table 4. Kinetic Data for the Stoichiometric Dioxygenation of $Cu^{II}(O_2Ncat)(tbeda)$ (**1**) and $Cu^{II}(O_2Ncat)(tmeda)$ (**2**)[a]

complex	$k_{98°C}$ ($\times 10^2$ s^{-1} mol^{-1} dm^3)	E_A (kJ mol^{-1})	$\Delta H^{\ddagger}$ (kJ mol^{-1})	$\Delta S^{\ddagger}$ (J mol^{-1} K^{-1})
1	4.63 ± 0.23	53 ± 6	51 ± 6	-137 ± 16
2	0.89 ± 0.16	88 ± 7	85 ± 7	-57 ± 19

[a] In 20 mL of DMF.

defined by two nitrogen atoms derived from the bidentate *N*,*N*,*N*′,*N*′-tetramethylethylenediamine ligand and two oxygen atoms of the bidentate 4-nitrocatecholate. The apical position is occupied by one oxygen atom of the 4-nitro group of the other $Cu^{II}(O_2Ncat)(tmeda)$ unit. The very small differences in the C−O ($\Delta = 0.038$ and 0.027 Å) and Cu−O ($\Delta = 0.039$ and 0.044 Å) bond lengths within each complex clearly indicate that the ligand coordinates with its two phenolate donors (4-nitrocatecholate) rather than with a phenolate and a quinone donor (4-nitrosemiquinone).

The slightly differing Cu−O bond lengths are caused by the asymmetry resulting from the NO_2 substitution. For complex $Cu^{II}(O_2Ncat)(tmeda)$, the copper−oxygen bond lengths [Cu−O2 = 1.934(5) Å, Cu−O1 = 1.907(4) Å] are somewhat longer than those found in the complex $Cu^{II}(O_2Ncat)(tbeda)$ [Cu−O2 = 1.926(5) Å, Cu−O1 = 1.888(5) Å]. With these increasing bond lengths the higher energy absorption bands (338 and 440 nm) are shifted to lower energies (i.e., higher wavelengths, 346 and 460 nm) in the order **1** < **2**, which can be explained by the ion (copper−catecholate) separation.

Electrochemistry. Redox potentials for complexes **1** and **2** are summarized in Table 2 (Figure S1). All values are given versus SCE. In *N*,*N*-dimethylformamide solution, complexes **1** and **2** display reversible one-electron redox processes (indicating the oxidation of the catecholate ligands) at $E_{1/2} = -50$ and 222 mV with $\Delta E = 113$ and 102 V, respectively. The more positive value for **2** is consistent with the formal substitution of the four methyl groups with benzyl groups in the ethylenediamine ligand. The study monitoring changes in the CV spectrum of **1** and **2** with the addition of $HClO_4$ showed a positive shift in the electrochemical oxidation potential, suggesting that the oxygenation of the protonated form is probably unfavored (Figure S2).

Stoichiometric Oxygenation of $Cu^{II}(L)(O_2Ncat)$ Complexes. After the characterization of the prepared complexes, their catechol 1,2-dioxygenase activity was examined. The (4-nitrocatecholato)copper complexes, $Cu^{II}(O_2Ncat)(tbeda)$ (**1**) and $Cu^{II}(O_2Ncat)(tmeda)$ (**2**), in DMF solutions are stable under anaerobic conditions and oxidized upon the addition of O_2, as shown in Figure 3.

In the absence of $HClO_4$, **1** and **2** were converted to a ring-opened product, the (2-nitromuconato)copper(II) complexes, as described in the Experimental Section. The GLC-MS analysis of the residue of the hydrolyzed complexes, after treatment with etheral diazomethane, shows the presence of the 4-nitromuconic acid diamide, 4-nitromuconic acid monoamide monomethylester, and furanon as oxygenated secondary products. The amide-containing products derived from the hydrolysis and amidation of the 4-nitromuconic acid by DMF, and the furanon is formed upon amidation of the unstable muconic acid anhydride as the Markovnikov product of γ-lactonization (Scheme 2). In the stoichiometric reactions, neither the products of the extradiol cleavage nor the products of the simple oxidation reaction, quinone, could be isolated as byproducts. Speier et al. reported an aerobic oxidation of a (phenanthrenediolato)copper(II) complex of tmeda, which is in a resonance of two valence tautomers of the (phenanthrenediolato)copper(II) and the (phenanthrenesemiquinonato)copper(I) states.[32] The (phenanthrenesemiquinonato)-copper(I) tautomer can bind a dioxygen molecule to form a dioxygen complex, which is decomposed to a ring-opened product. The reaction features and the products in that system are very similar to those in the aerobic oxidation of **1** and **2**. This indicates that the aerobic oxidation of **1** and **2** proceeds via dioxygen complexes similar to the (phenanthrenediolato)-(tmeda)Cu(II) system.

4-Nitrocatechol (O_2NcatH_2) has been found to be useful as a chromophoric probe of pH because of the distinct spectral features obtained when one or both of its protons are dissociated.[50] Coordinated 4-nitrocatechol to copper(II) in the presence of tbeda and tmeda resulted in a yellow color with absorption peaks at $\lambda_{max} = 283$, 338, 440 (**1**) and 283, 346 and 460 nm (**2**) in DMF. When $HClO_4$ was added to their solution, the yellow color disappeared. This suggested that the bidentate coordinated catecholate ligand may be protonated according to eq 1.

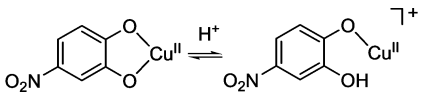

(1)

To check this and to prove the reversibility of the protonation, spectrophotometric titration of $Cu^{II}(O_2Ncat)(L)$ (**1**, **2**) complexes with $HClO_4$ was carried out. The spectra taken during the titration of **1** can be seen in Figure 4. It shows that both bands (283 and 440 nm) diminish upon the addition of $HClO_4$, exhibiting two isobestic points at 300 and 350 nm.

The plot of the absorbancies against the amount of $HClO_4$ added at both maxima shows inflection points at a $Cu^{II}(O_2Ncat)(tbeda)/HClO_4$ ratio of 1:1 (Figure 5). At a $Cu^{II}(O_2Ncat)(tbeda)/HClO_4$ ratio of 1:2, the copper catecholate complex is totally monoprotonated because of disappearance of the absorption peak at 440 nm in the electronic spectrum.

To check the reversibility of the protonation reaction, back-titration of the protonated complex with morpholine and NEt_3 were also carried out. The spectrophotometric back-titration showed the very same feature in the electronic spectra proving unequivocally the true reversible nature of the protonation of $Cu^{II}(O_2Ncat)(tbeda)$ (Figure 6). Similar results

(50) Tyson, C. A. *J. Biol. Chem.* **1975**, *250*, 1765.

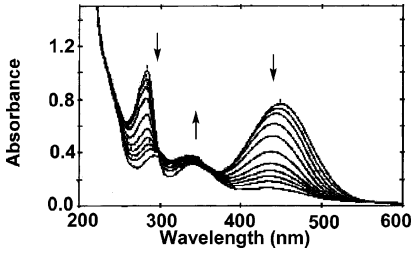

Figure 4. Spectra during the titration of $Cu^{II}(O_2Ncat)(tbeda)$ (**1**) with $HClO_4$ in DMF. $[Cu^{II}(O_2Ncat)(tbeda)] = 0.16$ mM, $[HClO_4] = 3.14$ mM (100 μL = 0.2 equiv), 25 °C.

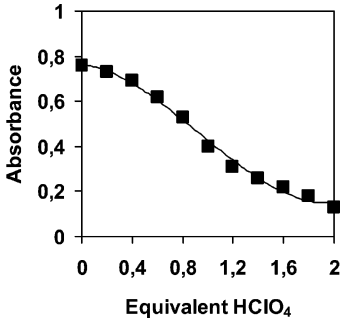

Figure 5. Dependences of the absorbances of $Cu^{II}(O_2Ncat)(tbeda)$ (**1**) as a function of added $HClO_4$ during the titration. $[Cu^{II}(O_2Ncat)(tbeda)] = 0.16$ mM, $[HClO_4] = 3.14$ mM (100 μL = 0.2 equiv.), 25 °C in DMF.

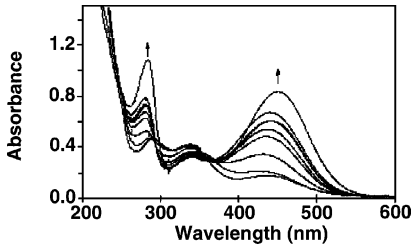

Figure 6. Dependences of the absorbances of $[Cu^{II}(O_2NcatH)(tbeda)]ClO_4$ (**1**) as a function of added morpholine during the titration. $[Cu^{II}(O_2Ncat)(tbeda)] = 0.16$ mM, [morpholine] = 3.14 mM, 25 °C in DMF.

were found for the $Cu^{II}(O_2Ncat)(tmeda)$ (**2**). On this basis, eq 1 could be established for the protonation reaction, and the equilibrium constants at 293 K were found to be 4200 (**1**) and 3500 (**2**) mol^{-1} dm^3 in DMF.

The product analysis for the aerobic oxidation of $Cu^{II}(O_2Ncat)(tbeda)$ (**1**) and $Cu^{II}(O_2Ncat)(tmeda)$ (**2**) in the presence of $HClO_4$ gave the same results as that of **1** and **2** in the absence of the acid. It suggests that the oxygenation of the protonated monodentate (catecholato)copper(II) complexes, $[Cu^{II}(O_2NcatH)(tbeda)]ClO_4$ (**3**) and $[Cu^{II}(O_2NcatH)(tmeda)]ClO_4$ (**4**), led also to the intradiol ring-cleaved dicarboxylates. These data support the assumption that the reaction of the differently coordinated catecholate ligand with dioxygen shows only dioxygenase-like activity in these cases.

Kinetic Measurements. Reactions of $Cu^{II}(O_2Ncat)(tbeda)$ (**1**) and $Cu^{II}(O_2Ncat)(tmeda)$ (**2**) with dioxygen were performed in DMF solutions at 80−125 °C, and the concentration change of $Cu^{II}(O_2Ncat)(L)$ (**1**, **2**) was followed by electronic spectroscopy measuring the absorbance of the reaction mixture at 440 and 460 nm, respectively. Experimental conditions are summarized in Tables S1 and S2. Figure 3 shows a typical experiment for $Cu^{II}(O_2Ncat)(tbeda)$

Scheme 2

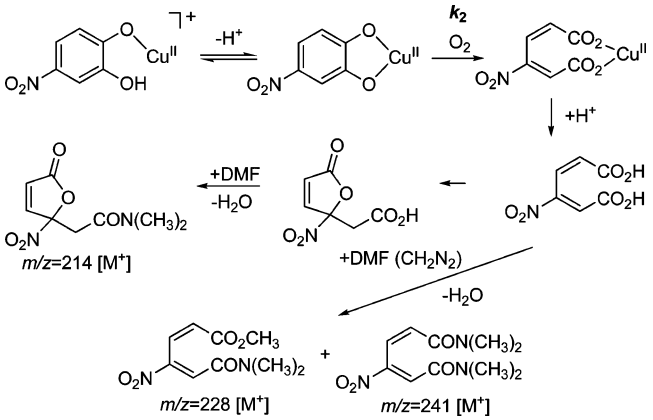

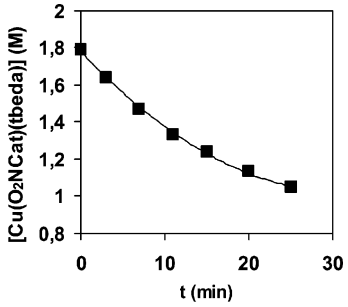

Figure 7. Time course of the oxygenation of $Cu^{II}(O_2Ncat)(tbeda)$ (**1**) in DMF at 92 °C: $[Cu^{II}(O_2Ncat)(tbeda)] = 0.18$ mM, $[O_2] = 7.95$ mM.

(**1**), resulting in a time-dependent disappearance of the 440 nm band concomitant with the appearance of a new band at 375 nm associated with the intradiol-cleaved product of 4-nitrocatecholate. There is a clear isobestic point at 405 nm, indicating that no build-up of optically detectable intermediates occurs between the bound 4-nitrocatecholate and its intradiol-cleaved product. To determine the rate dependence on the two reactants, oxygenation runs were performed at various initial $Cu^{II}(O_2Ncat)(L)$ (**1**, **2**) concentrations and different dioxygen pressures. A simple rate law for the reaction between $Cu^{II}(O_2Ncat)(L)$ (**1**, **2**) and O_2 is as shown in eq 2.

$$-\mathrm{d}[Cu(O_2Ncat)(L)]/\mathrm{d}t = k[Cu(O_2Ncat)(L)]^m[O_2]^n \quad (2)$$

Under pseudo-first-order conditions (constant dioxygen concentration) for the oxygenation of **1**, a typical time course and first-order plot are shown in Figure 7.

The first-order dependence of the reaction rate on **1** and **2** could also be confirmed by plotting the initial reaction rate $-\mathrm{d}[Cu^{II}(O_2Ncat)(L)]/\mathrm{d}t$ versus initial complex concentration (Figures 8 and S6).

Experiments made at different dioxygen pressures show that p_{O_2} appreciably influences the rate of the reaction in both cases. Kinetic measurements of the reaction rate respect to the dioxygen concentration indicate a first-order dependence (Figures 9 and S7).

On the basis of the results above, one can conclude that the reaction follows the rate law (eq 2) with $m = n = 1$, from which mean values of the kinetic constants k_{tbeda} of $4.63 \pm 0.23 \times 10^{-2}$ and k_{tmeda} of $0.89 \pm 0.16 \times 10^{-2}$ mol^{-1}

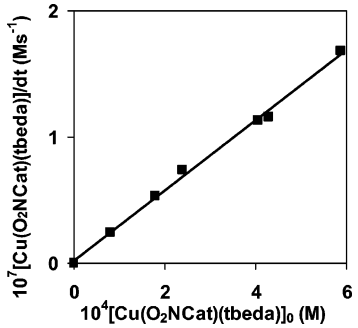

Figure 8. Plot of oxygenation rate of $Cu^{II}(O_2Ncat)(tbeda)$ (**1**) versus its initial concentration in DMF at 92 °C: $[O_2] = 7.95$ mM.

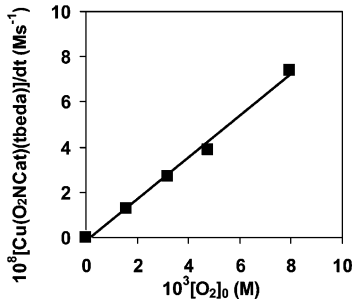

Figure 9. Plot of oxygenation rate of $Cu^{II}(O_2Ncat)(tbeda)$ (**1**) versus initial concentration of dioxygen in DMF at 92 °C: $[Cu^{II}(O_2Ncat)(tbeda)] = 0.24$ mM.

$dm^3\ s^{-1}$ at 371.16 K were obtained. The temperature-dependent reaction rate measurements for **1** and **2** in the range of 354.16−371.16 K resulted in a straight line in the Eyring plots, with activation parameters $\Delta H^{\ddagger} = 51 \pm 6$ kJ mol^{-1}, $\Delta S^{\ddagger}(371.16\ K) = -137 \pm 16$ J $mol^{-1}\ K^{-1}$ and $\Delta H^{\ddagger} = 85 \pm 7$ kJ mol^{-1}, $\Delta S^{\ddagger}(365.16\ K) = -57 \pm 19$ J $mol^{-1}\ K^{-1}$, respectively (Figures S8 and S9). Although activation parameters are often not discriminating factors in the recognization of the reaction pathway, the large negative entropy of activation ($\Delta S^{\ddagger}$) clearly indicates an associative mode of activation in the rate-determining step.

Kinetic studies on the oxygenation of the nitrocatecholate complex established a second-order overall rate expression, indicating that the rate-determining step must be bimolecular, namely, the reaction of $Cu^{II}(O_2Ncat)(L)$ with dioxygen (Scheme 2). Both reactions are entropy driven, and the redox properties of the nitrocatecholate complexes show that a higher electron density on the copper center increases its negative electrode potential, which leads to faster reaction rate.

Kinetic studies of the protonated copper catecholate complex $Cu(O_2NcatH)(tbeda)$ did not result in a clear picture. It seemed that to a large extent, deprotonation occurred at 92 °C to the unprotonated complex $Cu(O_2Ncat)(L)$, which has been oxygenated in an uncontrolled manner. However, bulk oxygenations of both $Cu(O_2Ncat)(L)$ and $Cu(O_2NcatH)(L)$ in DMF led to the same product to the intradiol ring-cleaved dicarboxylate, (2-nitromuconato)copper(II) complex.

The cyclic voltammograms of differentially protonated complex **2** with perchloric acid showed some positive shifts in their oxidation potentials (Figure S2). That means that the protonated complex may react with dioxygen more sluggishly or not at all. This statement is, however, not very solid, and the data above may also support the assumption that the reaction of the differently coordinated catecholate ligand with dioxygen shows dioxygenase-like activity. However, it cannot be excluded that because of the reversibility of the protonation of the nitrocatecholate ligand only the unprotonated ligand is reactive with dioxygen, since its presence is always secured as a result of the equilibrium between the two species. The data obtained could not make a secure differentiation in this respect.

Acknowledgment. Financial support of the Hungarian National Research Fund (OTKA T-043414), COST, Budaconsum Ltd., and Ulrich Trade Ltd. is gratefully acknowledged.

Supporting Information Available: Kinetic data, cyclic voltammograms of complexes **1** and **2**, MS spectra, tables containing atomic coordinates and equivalent isotropic displacement parameters, bond lengths, angles, anisotropic displacement parameters, hydrogen coordinates, and isotropic displacement parameters for complexes **1** and **2**, and crystallographic data in CIF format. This material is available free of charge via the Internet at http://pubs.acs.org.

IC062309A